Journal of Quantitative Spectroscopy & Radiative Transfer 276 (2021) 107929

Contents lists available at ScienceDirect

Journal of Quantitative Spectroscopy & Radiative Transfer

journal homepage: www.elsevier.com/locate/jqsrt

# The absorption spectrum of short-lived isotopic variant of water, $H_2{}^{15}O$: Tentative detection at the Earth's atmosphere

B.A. Voronin[a], M.V. Makarova[b], A.V. Poberovskii[b], A.D. Bykov[a], E.A. Dudnikova[c], J. Tennyson[d,*]

[a] V.E. Zuev Institute of Atmospheric Optics SB RAS, 1, sq. ac. Zuev, 634055, Tomsk, Russia
[b] Faculty of Physics, St. Petersburg State University, 198504 St. Petersburg, Russia
[c] Cancer Research Institute, Tomsk National Research Medical Center of the Russian RAS, Tomsk, Russia
[d] Department.of Physics and Astronomy, University College London, London, WC1E 6BT, UK

ARTICLE INFO

*Article history:*
Received 12 July 2021
Revised 4 September 2021
Accepted 5 September 2021
Available online 8 September 2021

*Keywords:*
$H_2{}^{15}O$
Spectrum
Line list
Water vapor
Atmospheric FTIR spectra

ABSTRACT

A calculated *infrared* vibration–rotation spectrum of isotopically modified water, $H_2{}^{15}O$, is presented. Oxygen-15 has a half-life of about 2 minutes and $H_2{}^{15}O$ may be formed in the atmosphere during thunderstorms as a result of photonuclear processes or when the atmosphere is irradiated by cosmic $\gamma$-rays. Variational nuclear motion calculations of vibrational and vibrational-rotational levels up to 25000 $cm^{-1}$ and up to $J = 10$ in angular momentum are performed within the framework of the Born-Oppenheimer approximation using an accurate water potential function. The line shape parameters for $H_2{}^{15}O$ are estimated. Spectral ranges that are promising for the detection of $H_2{}^{15}O$ in the atmosphere are identified and a search for spectral signatures conducted. A spectral feature is tentatively assigned to the $7_{52}$ (0 1 0) - $6_{43}$ (0 0 0) line of $H_2{}^{15}O$.



## 1. Introduction

Studies of water vapor spectra and determination of spectral line parameters for the water molecule, both for the parent $H_2{}^{16}O$ isotopologue and isotopic modifications such as $HD^{16}O$ $H_2{}^{17}O$ and $H_2{}^{18}O$, underpin numerous astrophysical, atmospheric and technological applications. Detailed spectroscopic data on these stable water isotopologues are available from data banks, for example, HITRAN [1], GEISA [2] and ExoMol [3]. Furthermore, numerous studies have been carried out, both experimentally and theoretically, on other stable isotopologues of water containing $^{17}O$, $^{18}O$ and/or deuterium. Critical analysis of a large array of measured and calculated data was carried out within the framework of a IUPAC task group [4,5]. Measurements and calculations have also been conducted on radioactive, tritium-containing water, see SPECTRA [6] and Down et al. [7].

A range of unstable, radioactive isotopes of oxygen are known; the longest lived of these is $^{15}O$ which has a half-life of about 2.1 minutes [8], which makes it sufficiently long-lived to be detected using spectroscopic techniques. Cosmic gamma radiation is known to be source of the $H_2{}^{15}O$ radioactive water isotopologue in the atmosphere [9]; $H_2{}^{15}O$ can arise as a result of photonuclear processes such as $^{16}O + \gamma \rightarrow {}^{15}O + n$. The $H_2{}^{15}O$ isotopologue is thought to be formed in thunderstorms (see, for example, [10,11] and references here). Monte Carlo simulations have shown that, due to the action of intense bremsstrahlung associated with runaway relativistic electrons, various isotopic modifications of hydrogen, nitrogen, oxygen and carbon are formed in the lightning discharge channel, which lead to observable features in the emission of photons [11]. In general, high-energy electrons, bremsstrahlung, are capable of knocking neutrons out of the nuclei of atmospheric species such as the $^{14}N_2$ and $^{16}O_2$ molecules and of atomic argon $^{40}Ar$, as well as of atoms on surfaces, e.g. $^{27}Si$, $^{26}Al$, $^{56}Fe$ and $^{16}O$ [10].

Other important, practical applications of radioactive isotopes of water, are found in biology [12] and medicine, where $^{15}O$, along with other positron emitting nuclides ($^{18}F$, $^{11}C$, $^{13}N$), is used when performing positron emission computed tomography [13–15]. Furthermore, radio-pharmaceutical preparations containing oxygen-15 ($^{15}O_2$, $C^{15}O_2$, $H_2{}^{15}O$) are the main ones for the determination of cerebral perfusion [16]. This is primarily due to the short half-life of this radionuclide (~ 2.1 min), which is comparable to the time frame of the oxygen utilization processes occurring in the body [13]. The method of administration and the research procedure relies on the use of a suitable radio-pharmaceutical: $H_2{}^{15}O$ is usually

* Corresponding author.
*E-mail address:* j.tennyson@ucl.ac.uk (J. Tennyson).

https://doi.org/10.1016/j.jqsrt.2021.107929

administered intravenously. Since water occurs naturally in living organisms, the use of $H_2{}^{15}O$ does not cause side effects. The propagation of water is monitored by detecting $\gamma$-rays with an energy of about 0.511 MeV which are created by annihilation of positrons [17].

As far as we are aware, there are no previous measurements or calculations of vibrational - rotational energy levels or spectra of $H_2{}^{15}O$. Measuring the spectrum of $H_2{}^{15}O$ is challenging due to its instability, radioactivity and short half-life. Therefore, it seems useful to calculate the spectra building on information available for stable water isotopologues. The purpose of this work is to calculate both the absorption spectrum of $H_2{}^{15}O$, based on use of a high-accuracy potential energy function, and to determine which spectral ranges are the most promising for its detection in the Earth's atmosphere.

## 2. Calculation

We obtain the necessary spectral information for $H_2{}^{15}O$ using two separate methods. The first method is the calculation of vibrational-rotational levels, centers and intensities of spectral lines, based on a high-precision potential energy surface and dipole moment, using the DVR3D package [18]. This method uses the Born-Oppenheimer approximation, in which the mass dependence of the potential energy surface is ignored. The second method exploits the fact that the substitution of the oxygen isotope refers to the case of substitution of heavy atoms. In this case, a small parameter appears in the problem, namely the relative change in mass during isotope substitution. The application of perturbation theory makes it possible to represent the isotopic shift of an individual level in the form of a series in powers of $\mu=(m'-m)/m$, where $m'$ and $m$ are the masses of the substituting and substituted isotopes, respectively. In this case it is possible, using the experimental values of the levels of the stable isotopologues $H_2{}^{X}O$ (X = 16, 17, 18) from the list of empirical levels provided by a IUPAC task group [4,5], to determine the coefficients of the second-degree interpolating polynomial and to extrapolate the energy, determining the values of the levels for X = 15. The possibility of using estimates of isotope substitution to calculate energy levels and even spectra has been known for a long time; see the monograph of 1985 [19] or a recent paper [20].

For these calculations we take the oxygen isotope masses from [8]: 15.0030656 Da for $^{15}O$, and 15.99491461960, 16.9991317566, 17.9991596128 Da for $^{16}O$, $^{17}O$, $^{18}O$, respectively. In this case, the parameters *μ(16 -> X)* are equal -0.0661097569019, 0.0590746134202, and 0.1113521428953 for X = $^{15}O$, $^{17}O$, $^{18}O$. To estimate vibration energy levels of $H_2{}^{15}O$, we use empirical $H_2{}^{16}O$, $H_2{}^{17}O$ and $H_2{}^{18}O$ energy levels from the recent W2020 compilation [21]. For each level a set of linear equations:

$$^{17}E_V - {}^{16}E_V = x_1^v \mu(16 \to 17) + x_2^v \mu(16 \to 17)^2 \quad (1)$$

$$^{18}E_V - {}^{16}E_V = x_1^v \mu(16 \to 18) + x_2^v \mu(16 \to 18)^2 \quad (2)$$

where

$$\mu(16 \to 17) = \frac{m_{17} - m_{16}}{m_{17}},\ \mu(16 \to 18) = \frac{m_{18} - m_{16}}{m_{18}}, \quad (3)$$

has been solved giving $x_1{}^v$ and $x_2{}^v$ . The vibrational energy levels of the $H_2{}^{15}O$ isotopologue are then calculated using formula:

$$^{m}E_v = {}^{16}E_v + x_1^v \mu(16 \to m) + x_2^v \mu(16 \to m)^2 \quad (4)$$

with $m$= 15.

Our earlier calculation of the VoTe $H_2{}^{16}O$ line list [22] was performed using the potential energy surface (PES) of Bubukina et al. [23] and the LTP2011 dipole moment surface [24]; the DVR3D software package [18] was used for the calculations. In order to check whether it is possible to carry out calculations of $H_2{}^{15}O$ isotopologues using the same DVR3D technique, test calculations of the vibrational and vibrational - rotational levels of $H_2{}^{17}O$ and $H_2{}^{18}O$ were carried out for small values of the quantum number *J*. Typical results are presented in Table 1. The same procedure was used, as in [22], except that the mass of the oxygen atom, which was replaced by the appropriate isotopic mass from [8]. It was found that the deviations of the calculated levels from the empirical ones did not exceed 0.1 $cm^{-1}$ for all vibrational levels below 10000 $cm^{-1}$. Based on this, we believe that the possible error in predicting energy levels for other isotopologues of $H_2{}^{X}O$ without accounting for deviations from the Born-Oppenheimer approximation, will be approximately the same, that is, 0.1 $cm^{-1}$ or better.

Table 1 gives the vibrational quantum numbers, the values of the energy levels according to the data [4,5,21] and the difference between the values of the energy levels in $cm^{-1}$. The predictions made using two different methods show good agreement with each other and the empirical data.

## 3. Calculation of the $H_2{}^{15}O$ absorption spectrum and estimation of line parameters

Energy levels, line centers, and line intensities were calculated up to $J$ = 10 for $H_2{}^{15}O$. The calculations were carried out using DVR3D and, as in the calculation of the VoTe $H_2{}^{16}O$ line list [22], the PES of Bubukina et al. [23] and the LTP2011 dipole moment surface [24] were used. The calculations were performed on the "amun" cluster at UCL.

The assignment of approximate quantum numbers to energy levels was not carried out. An exception is the total angular momentum *J*, which varies from 0 to 10. The calculation is performed for room temperature (296 K).

The line half-widths were estimated for $H_2{}^{15}O$ in the same way as previously done for $H_2{}^{16}O$ in [25]. That is, previously published estimates of the *J*-dependence for $\gamma_{self}$ and the *JJ*-dependence of $\gamma_{air}$ were used [25]. The results are presented in Table 2 in a format similar to the HITRAN database. The isotopologue number is denoted as 18, since, in HITRAN, 11 is $H_2{}^{16}O$, 12 is $H_2{}^{18}O$, 13 is $H_2{}^{17}O$, 14 is $HD^{16}O$, ...., $D_2{}^{16}O$ is 17, and so the new entry $H_2{}^{15}O$ can be designated 18.

Table 2 gives "18" - the isotopologue index, frequency in $cm^{-1}$, intensity at 296 K (at 100% abundance) in cm/molecule, Einstein coefficient, coefficients of air broadening, self-broadening, value of the lower energy level, temperature dependence coefficient, shift (assumed zero in all cases), and vibrational and rotational quantum numbers. See the file fort.36.h215o_I30.296K-HW.dat at ftp://ftp.iao.ru/pub/VTT/H215O/SpectraH215O/ which contains a full line list of 115523 lines.

## 4. On the delectability of $H_2{}^{15}O$ in atmospheric infrared transmission spectra

To study the possibility of retrieving $H_2{}^{15}O$ from atmospheric IR (infrared) transmission spectra, the following information and data were used:

1 The spectroscopic database (file fort.36.h215o_I30.296K-HW.dat) containing data on the parameters of the spectral lines of $H_2{}^{15}O$;
2 The archive of FTIR (Fourier transform infrared) spectra of direct solar radiation recorded using a high-resolution FTS (Fourier transform spectrometer) Bruker IFS 125HR installed at the St. Petersburg station (Faculty of Physics, St. Petersburg State University, a member of IRWG of NDACC network), https://www.ndaccdemo.org/stations/st-petersburg-russian-federation) [26,27]. The typical res-

**Table 1**
Vibrational energy levels, in $cm^{-1}$, of the water isotopologues $H_2{}^{15}O$, $H_2{}^{16}O$, $H_2{}^{17}O$, $H_2{}^{18}O$ calculated using two methods: DVR3D and quadratic interpolation using the mass parameter μ, (VVV) "DVR3D- extrapolated" is the difference between the two predictions.

| | $H_2{}^{15}O$ | $H_2{}^{16}O$ | $H_2{}^{17}O$ | $H_2{}^{18}O$ |
|---|---|---|---|---|
| (010) empirical [28] | | 1594.7462 | 1591.3257 | 1588.2759 |
| (010) DVR3D | 1598.5385 | 1594.7469 | 1591.3299 | 1588.2831 |
| (010) extrapolated | 1598.5419 | 1594.7462 | 1591.3257 | 1588.2759 |
| (010) DVR3D- extrapolated | -0.0034 | 0.0006 | 0.0042 | 0.0071 |
| (020) empirical [28] | | 3151.6299 | 3144.9807 | 3139.0500 |
| (020) DVR3D | 3158.9730 | 3151.6043 | 3144.9623 | 3139.0389 |
| (020) extrapolated | 3159.0048 | 3151.6299 | 3144.9807 | 3139.0500 |
| (020) DVR3D- extrapolated | -0.0318 | -0.0257 | -0.0184 | -0.0112 |
| (100) empirical [28] | | 3657.0531 | 3653.1423 | 3649.6853 |
| (100) DVR3D | 3661.3702 | 3656.9965 | 3653.0930 | 3649.6423 |
| (100) extrapolated | 3661.4352 | 3657.0531 | 3653.1423 | 3649.6853 |
| (100) DVR3D - extrapolated | -0.0650 | -0.0566 | -0.0493 | -0.0430 |
| (110) empirical [28] | | 5234.9746 | 5227.7056 | 5221.2440 |
| (110) DVR3D | 5243.0313 | 5234.9312 | 5227.6707 | 5221.2279 |
| (110) extrapolated | 5243.0680 | 5234.9746 | 5227.7056 | 5221.2440 |
| (110) DVR3D - extrapolated | -0.0367 | -0.0434 | -0.0349 | -0.0161 |
| (120) empirical [28] | | 6775.0929 | 6764.7256 | 6755.5108 |
| (120) DVR3D | 6786.5649 | 6775.0329 | 6764.6782 | 6755.4752 |
| (120) extrapolated | 6786.6373 | 6775.0929 | 6764.7256 | 6755.5108 |
| (120) DVR3D - extrapolated | -0.0725 | -0.0600 | -0.0474 | -0.0356 |
| (200) empirical [28] | | 7201.5400 | 7193.2448 | 7185.8777 |
| (200) DVR3D | 7210.7306 | 7201.4991 | 7193.2190 | 7185.8648 |
| (200) extrapolated | 7210.7856 | 7201.5400 | 7193.2448 | 7185.8777 |
| (200) DVR3D - extrapolated | -0.0550 | -0.0409 | -0.0258 | -0.0128 |
| (002) empirical [28] | | 7445.0456 | 7431.0769 | 7418.7234 |
| (002) DVR3D | 7460.5632 | 7444.9575 | 7431.0083 | 7418.6632 |
| (002) extrapolated | 7460.6892 | 7445.0456 | 7431.0769 | 7418.7234 |
| (002) DVR3D - extrapolated | -0.1260 | -0.0881 | -0.0686 | -0.0603 |
| (012) empirical [28] | | 9000.1374 | 8982.8692 | 8967.5629 |
| (012) DVR3D | 9019.3063 | 9000.0383 | 8982.7875 | 8967.4979 |
| (012) extrapolated | 9019.4266 | 9000.1374 | 8982.8692 | 8967.5629 |
| (012) DVR3D - extrapolated | -0.1203 | -0.0991 | -0.0817 | -0.0650 |
| (102) empirical [28] | | 10868.8758 | 10853.5053 | 10839.9560 |
| (102) DVR3D | 10886.0415 | 10868.7987 | 10853.4517 | 10839.9207 |
| (102) extrapolated | 10886.1514 | 10868.8758 | 10853.5053 | 10839.9560 |
| (102) DVR3D - extrapolated | -0.1099 | -0.0771 | -0.0536 | -0.0353 |

**Table. 2**
Portion of the calculated of $H_2{}^{15}O$ line list for 296 K.

| Iso | Freq. $cm^{-1}$ | Intensity cm/molec | A, $s^{-1}$ | $\gamma_{air}$ $cm^{-1}$ $atm^{-1}$ | $\gamma_{self}$ | E low $cm^{-1}$ | Shift | $v_1$ $v_2$ $v_3$ Upper | J Ka Kc upper | $v_1$ $v_2$ $v_3$ lower | J Ka Kc lower |
|---|---|---|---|---|---|---|---|---|---|---|---|
| 18 | 0.153696 | 0.939E-29 | 0.5E-10 | 0.0870 | 0.523 | 1927.454590 | 0.0 | -2 -2 -2 | 4 -2 -2 | -2 -2 -2 | 5 -2 -2 |
| 18 | 0.522376 | 0.391E-27 | 0.3E-08 | 0.0925 | 0.563 | 1912.943726 | 0.0 | -2 -2 -2 | 3 -2 -2 | -2 -2 -2 | 4 -2 -2 |
| 18 | 0.583541 | 0.149E-27 | 0.3E-08 | 0.0870 | 0.523 | 2136.386963 | 0.0 | -2 -2 -2 | 4 -2 -2 | -2 -2 -2 | 5 -2 -2 |
| 18 | 0.883302 | 0.939E-29 | 0.5E-08 | 0.0561 | 0.290 | 2910.526855 | 0.0 | -2 -2 -2 | 10 -2 -2 | -2 -2 -2 | 9 -2 -2 |
| 18 | 1.060925 | 0.931E-24 | 0.6E-08 | 0.0811 | 0.443 | 447.308197 | 0.0 | -2 -2 -2 | 6 -2 -2 | -2 -2 -2 | 5 -2 -2 |
| 18 | 1.944495 | 0.910E-26 | 0.'E-06 | 0.0924 | 0.523 | 1824.052612 | 0.0 | -2 -2 -2 | 4 -2 -2 | -2 -2 -2 | 3 -2 -2 |

olution of the recorded atmospheric FTIR spectra is 0.005 $cm^{-1}$.

3 The archive containing dates and times of thunderstorm activity observed in the vicinity of St. Petersburg during 2011-2020. (http://www.meteocenter.asia/ts.php?Mon=07&Year=2014&p=26063).

We surmise that FTIR spectra recorded during thunderstorm activity could have an increased chance of registering $H_2{}^{15}O$ lines in the atmospheric transmittance spectra.

Our study consists of three steps:

- first, selecting spectral intervals in the mid IR spectral band which could be potentially used for for identification purposes. For this, we used experimental FTIR spectra to detect spectral intervals where most intensive $H_2{}^{15}O$ lines (for the information about position and intensity of $H_2{}^{15}O$ lines we used the file fort.36.h215o_I30.296K-HW.dat file) do not coincide with the regions of full atmospheric absorption. As a result, the spectral region around the $H_2{}^{15}O$ line having its center at 1973.5228 $cm^{-1}$ and room-temperature intensity of $7 \times 10^{-21}$ cm/molecule was chosen for further processing and detailed analysis;
- second, processing of the set of FTIR spectra acquired during 2011-2019 at the St.Petersburg station (SPbU) using the F2 optical filter and InSb detector (totally, about 4800 spectra). The FTIR spectra were processed using the SFIT4 software [28] in the spectral range 1973.490 - 1973.565 $cm^{-1}$. The center of the selected $H_2{}^{15}O$ line (1973.5228 $cm^{-1}$) lies on the wing of an intense $CO_2$ line (see Fig. 1). The processing procedure includes the retrieval of the following atmospheric trace gases: $COF_2$, $CO_2$, $O_3$, $N_2O$, $CH_4$, and $H_2O$. We used the HITRAN2012 database [1] for spectral information for all these species in the range 1973.490 - 1973.565 $cm^{-1}$. For the Fraunhofer lines (solar lines), we used the database [29] which is distributed together with SFIT4 software. *A priori* gas profiles were set based on the simulations of the WACCM model [30]. An example of

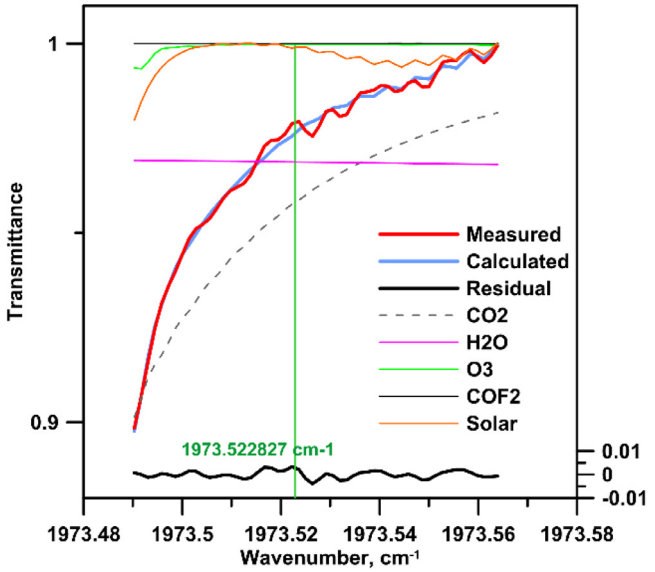


**Fig. 1.** An example of fitting the calculated spectrum (blue curve) to the measured one (red curve) (06/10/2011, 09:04:48 UTC), as well as the difference between them (black curve). Thin colour lines - the results of calculating the transmission of $COF_2$, $CO_2$, $O_3$ and $H_2O$, as well as the solar spectrum (in transmission units).

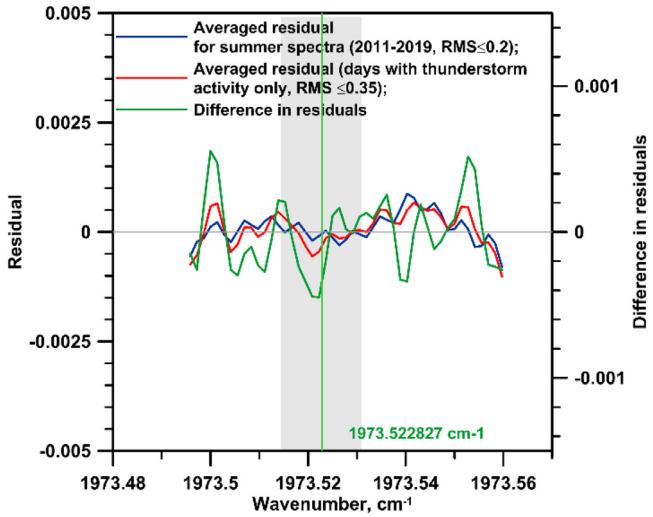


**Fig. 2.** Results of residual averaging (difference between measured and calculated spectra) for two subsets of spectra - "full" with RMS≤0.2% (blue line) and "thunderstorm" with RMS≤0.35% (red line). The difference between these residuals is shown by the green line.

fitting the simulated spectrum to a measured one (06/10/2011, 09:04:48 UTC) is given in Fig. 1. Fig. 1 also shows the calculated transmittances of $CO_2$, $O_3$, $H_2O$ and $COF_2$, as well as the solar spectrum (in transmittance units). The difference (residual) between simulated and measured spectra for 06/10/2011, 09:04:48 UTC is given in Fig. 1. The RMS (root mean square) value of this difference is of 0.31%.

- third, comparative analysis of the results of the FTIR spectra processing for two subsets of the full set of spectra (2011-2019). The first subset ("thunderstorm") included the spectra recorded during the days when thunderstorm activity was observed for the St.Petersburg area. In total for 2011-2019 we selected 360 spectra for 58 days. Usually the period when thunderstorms are observed in St.Petersburg lasts about five months (from May to September). The second subset ("full") includes all spectra measured during the period from May to September (2011-2019), except for the days from the first sample (i.e., days with thunderstorm activity). This approach was based on the hypothesis that thunderstorms can cause a short-term increase in the content of $H_2{}^{15}O$ in the atmosphere. Therefore, comparison of the processing results for the two selected subsets of FTIR spectra could increase our chance to detect lines of the short-lived isotopologue $H_2{}^{15}O$ in atmospheric spectra. Since it is assumed that the content of $H_2{}^{15}O$ in the atmosphere is very small or even negligible, the processing of a single FTIR spectrum, which, in our case, has a relatively low signal-to-noise ratio of ~ 300-500, may not lead to the desired result, namely a reliable determination of the total content of $H_2{}^{15}O$ in the atmosphere. Therefore, we have chosen an approach based on the accumulation of information. This can, on a qualitative level, answer the question of the possibility of detection (and, in fact, the existence) of the $H_2{}^{15}O$ spectral line in the atmosphere in the region around 1973.5228 $cm^{-1}$. For this, additional filtering using the RMS level was applied to both subsets: in the first case, spectra with RMS values exceeding 0.35% were filtered out; in the second - with RMS values above 0.2%. Further, for both subsets, the residual (the difference between the measured and calculated spectra) was averaged over the corresponding subsets of spectra ("thunderstorm" and full). The resulting average residuals for both subsets are shown in Fig. 2.

The same figure shows the difference between these residuals, which has a region of negative values in the region of the $H_2{}^{15}O$ line (highlighted in Fig. 2 by a light gray stripe), which may indicate the presence in this spectral range of a spectral line (or lines) unaccounted for in the calculations, which manifests itself in specific atmospheric conditions (in our case, in the presence of thunderstorm activity). However, it should be noted that, first, the minimum of this region (1973.521 $cm^{-1}$) does not show an exact coincidence with the position of the center of the $H_2{}^{15}O$ line (1973.5228 $cm^{-1}$, green vertical line in Fig. 2.). Second, this minimum is ~ 0.04% of the total transmission of the atmosphere, which is a very small value that is extremely difficult to detect under atmospheric conditions. Third, in the range of wave numbers 1973.515-1973.530 $cm^{-1}$, there are a number of weak lines of atmospheric gases: three $O_3$ lines (1973.5171 $cm^{-1}$ (main isotope), 1973.52147 $cm^{-1}$ and 1973.52414 $cm^{-1}$ (33 isotope)); two $COF_2$ lines (1973.5183 $cm^{-1}$ and 1973.5198 $cm^{-1}$); $CO_2$ line (1973.520918 $cm^{-1}$) and $N_2O$ line (1973.525030 $cm^{-1}$). We need to consider that thunderstorm activity brings about a short-term increase in the ozone content of the troposphere, leading in turn to an increase in absorbance of weak ozone lines. These three ozone lines in the range of 1973.515-1973.530 $cm^{-1}$ could therefore have an effect on our analysis.

Finally, our analysis does not allow us to make the unambiguous conclusion that the region of negative values of the residual difference (Fig. 2) is due to the presence of the theoretically predicted spectral line of the short-lived isotopologue $H_2{}^{15}O$ centered at 1973.5228 $cm^{-1}$. Nevertheless, the spectral interval 1973.475 - 1973.575 $cm^{-1}$ proposed in current study might be promising for further investigations, for example, using high resolution laboratory experiments and a thorough analysis of the atmospheric FTIR spectra recorded at IRWG NDACC stations having more favorable geographic/climatic conditions.

## 5. Assignments of the $H_2{}^{15}O$ 1973.522827 $cm^{-1}$ line

The $H_2{}^{15}O$ absorption line at 1973.5228 $cm^{-1}$ with intensity ~ $7 \times 10^{-21}$ molecules/cm corresponds to a transition from $J$=6 to $J$=7. Because the symmetry types and energy of the upper and lower levels are also known then by comparing with VoTe ($H_2{}^{16}O$) line list, one can easily found that this line can be assigned to (0 1

0) [7 5 2] ← (0 0 0) [6 4 3] vibration – rotation transition. These assignments is confirmed by the isotopic shift of the line of (0 1 0) [7 5 2] ← (0 0 0) [6 4 3].

## 6. Conclusion

We have calculated vibrational - rotational energy levels, line positions and strengths of a radioactive isotopologue of water - the $H_2{}^{15}O$ molecule. The calculations were based on a high-precision potential energy surface [23] and dipole moment surface [24], and assume that corrections due to deviations from the Born–Oppenheimer approximation and other mass-dependent factors are small. The calculations were carried out in two different ways, the DVR3D method and quadratic extrapolation based on the experimental levels of $H_2{}^{16}O$, $H_2{}^{17}O$ and $H_2{}^{18}O$. The results of these two calculations are in satisfactory agreement with each other.

Our analysis of atmospheric FTIR spectra does not permit us to conclude that the spectral line of the short-lived istopologue $H_2{}^{15}O$ centered at 1973.5228 $cm^{-1}$ can be reliably detected in the atmosphere. Under conditions of thunderstorm activity, a short-term increase of different components occur, including the tropospheric ozone, which, in turn, can lead to an increase of absorption near this $H_2{}^{15}O$ line. Nonetheless, the spectral range 1973.490 - 1973.565 $cm^{-1}$ can be considered as promising for detection of $H_2{}^{15}O$ in the earth's atmosphere. Additional studies are needed, including, perhaps, laboratory experiments, as well as further analysis of atmospheric FTIR spectra recorded at IRWG NDACC stations with more advantageous geographic location.

## Author Statement

B.A. Voronin performed the investigation, made the original draft of the manuscript is responsible for data curation; M.V. Makarova prepared the section of the manuscript concerning the detectability in the atmosphere, performed analysis of thunderstorm activity, and performed analysis of the atmospheric FTIR spectra. A.V. Poberovskii provided the maintenance of FTIR observations. A.D. Bykov and J. Tennyson provided the methdology; J. Tennyson provided the final draft of the manuscript.

## Declaration of Competing Interest

None of the authors declare a conflict of interest.

## Acknowledgments

The authors are grateful to Prof. S.N. Yurchenko. This work was financially supported by budget project of Zuev V.E. IAO SB RAS and the UK Natural Environment Research Council grant NE/T000767/1. The FTIR spectra were recorded using Bruker IFS 125HR spectrometer maintained by the Research Centre GEOMODEL of St. Petersburg State University (http://geomodel.spbu.ru/). The analysis of FTIR spectra was carried out at the Atmospheric Physics Department (Faculty of Physics, SPbU).

## References

[1] Rothman LS, Gordon IE, Babikov Y, Barbe A, Benner DC, Bernath PF, et al. J Quant Spectrosc Radiat Transf 2013;130:4.
[2] Jacquinet-Husson N, Armante R, Scott NA, Chédin A, Crépeau L, Boutammine C, Bouhdaou iA, Crevoisier C, Capelle V, Boonne C, Poulet-Crovisier N, Barbe A, Benner CD, Boudon V, Brown LR, Buldyreva J, Campargue A, Coudert LH, Devi VM, Down MJ, Drouin BJ, Fayt A, Fittschen C, Flaud J-M, Gamache RR, Harrison JJ, Hill C, Ø Hodnebrog, HuS-M Jacquemart, D Jolly, A Jiménez, E Lavrentieva, NN Liu, A-W Lodi, L Lyulin, OM Massie, ST Mikhailenko, S Müller, HSP Naumenko, OV Nikitin, A Nielsen, CJ Orphal, J Perevalov, VI Perrin, A Polovtseva, E Predoi-Cross, A Rotger, M Ruth, AA Yu, SS Sung, K Tashkun, SA Tennyson, J Tyuterev, VlG Vander Auwera J, Voronin BA, Makie AJ. Mol Spectrosc 2016;327:31.
[3] Tennyson J, Yurchenko SN, Al-Refaie AF, Clark VHJ, Chubb KL, Conway EK, et al. The 2020 release of the ExoMol database: molecular line lists for exoplanet and other hot atmospheres. J Quant Spectrosc Rad Transf 2020;255:107228. doi:10.1016/j.jqsrt.2020.107228.
[4] Tennyson J, Bernath PF, Brown LR, Campargue A, Carleer MR, Császár AG, et al. IUPAC critical evaluation of the rotational–vibrational spectra of water vapor. Part I—Energy levels and transition wavenumbers for $H_2{}^{17}O$ and $H_2{}^{18}O$. J Quant Spectrosc Radiat Transf 2009;110:573–96.
[5] Tennyson J, Bernath PF, Brown LR, Campargue A, Császár AG, Daumont L, et al. Mizus I.I. IUPAC critical evaluation of the rotational–vibrational spectra of water vapor, Part III: Energy levels and transition wavenumbers for $H_2{}^{16}O$. J Quant Spectrosc Radiat Transf 2013;117:29–58.
[6] Mikhailenko SN, Babikov YuL, Golovko VF. Information-calculating system spectroscopy of atmospheric gases. The structure and main functions. Atmos Ocean Opt 2005;18:685–95. http://spectra.iao.ru/molecules.
[7] Down MJ, Tennyson J, Hara M, Hatano Y, Kobayashi K. Analysis of a tritium enhanced water spectrum between 7200 - 7245 $cm^{-1}$ using new variational calculations. J Molec Spectrosc 2013;289:35–40.
[8] Wang M, Audi G, Wapstra AH, Kondev FG, MacCormick M, Xu X, et al. The Ame2012 atomic mass evaluation (II). Tables, graphs, and references. Chin Phys C 2012;36:7. doi:10.1088/1674-1137/36/12/003.
[9] Gann AV, Gann VV, Pugachev GD, Shapoval II, Shapoval IA, Shestakova VS. Dependence of rate of 13N and 15O radionuclides production in air from the maximal energy and the spectrum of bremsstrahlung. Probl Atom Sci Technol 2010(53):P.178–P.180 № 2. Series: Nuclear Physics Investigations(in Russian).
[10] Babich LP. Thunderous neutrons. Phys Usp 2019;62:976–99. doi:10.3367/UFNe.2018.12.038501.
[11] Ortega PG. Isotope production in thunderstorms. J Atmos Solar–Terrestrial Phys 2020;208:105349. doi:10.1016/j.jastp.2020.105349.
[12] Kobayashi M, Kiyono Y, Maruyama R, Mori T, Kawai K, Okazawa H. Development of an $H_2{}^{15}O$ steady-state method combining a bolus and slow increasing injection with a multiprogramming syringe pump. J Cereb Blood Flow Metab 2011;31:527–34. doi:10.1038/jcbfm.2010.122.
[13] Powers WJ, Stabin M, Howse D, Eichung JO, Herscovitch P. Radiation absorbed dose estimatesfor oxygen-15 radiopharmaceuticals ($H_2{}^{15}O$, $C^{15}O$, $O^{15}O$) in newborn infants. J Nucl Med 1988;29:1961–70.
[14] Chernov VI, Dudnikova EA, Goldberg VE, Kravchuk TL, Danilova AV, Zelchan RV, et al. Positron emission tomography in the diagnosis and monitoring of lymphomas. Med Radiol Radiation Saf 2018;63:41–50. doi:10.12737/article_5c0b8d72a8bb98.40545646.
[15] Chernov VI, Goncharova NM, Goldberg VE, Dudnikova EA, Zelchan RV, Medvedeva AA, et al. The value of PET/CT in the diagnosis, stading and monitoring of colorectal cancer. Siberian J Oncology 2019;18:67–77. doi:10.21294/1814-4861-2019-18-4-67-77.
[16] Saha GB, MacIntyre WJ, Go RT. Radiopharmaceuticals for brain imaging. Sem. Nucl. Med. 1994;24:324–49. doi:10.1016/s0001-2998(05)80022-4.
[17] Dowsett D. Radiological sciences dictionary: keywords, names and definitions. 1st Edition. London: Hodder Arnold; 2009. xiv, 359 p.: ill. DOI https://doi.org/10.1201/b13300.
[18] Tennyson J, Kostin MA, Barletta P, Harris GJ, Polyansky OL, Ramanlal J, et al. Computer Phys Comm 2004;163:85.
[19] Bykov AD, Makushkin Yu S, Ulenikov ON. Isotope substitution in polyatomic molecules. In: Kabanov MV, editor. Science. Novosibirsk: SB RAS, Sibirisn Department; 1985. p. 1–159. (at Russian).
[20] Loëte M, Richard C, Boudon V. Isotopic relations for tetrahedral and octahedral molecules. J Mol Struct 2020;V. 1206:P.127729. doi:10.1016/j.molstruc.2020.127729.
[21] Furtenbacher T, Tobias R, Tennyson J, Polyansky OL, Kyuberis AA, Ovsyannikov RI, et al. W2020: a database of validated rovibrational experimental transitions and empirical energy levels Part II. $H_2{}^{17}O$ and $H_2{}^{18}O$ with an update to $H_2{}^{16}O$. J Phys Chem Ref Data 2020;49:043103.
[22] Voronin BA, Tennyson J, Lodi L, Kozodoev AV. The VoTe room temperature $H_2{}^{16}O$ line list up to 25 000 $cm^{-1}$. Opt Spectrosc 2019;127:967–73.
[23] Bubukina II, Zobov NF, Polyansky OL, Shirin SV, Yurchenko SN. Opt Spectrosc 2011;110:160.
[24] Lodi L, Tennyson J, Polyansky OL. J Chem Phys 2011;135:034113.
[25] Voronin BA, Lavrentieva NN, Mishina TP, Chesnokova TYu, Barber MJ, Tennyson J. J Quant Spectrosc Radiat Transfer 2010;111:2308.
[26] Makarova MV, M Timofeev Yu, Poberovskii AV, Kh Imkhasin Kh, Osipov SI, Makarov BK. Analysis of methane total column variations in the atmosphere near St. Petersburg using ground-based measurements and simulations. Izvestiya Atmos Ocean Phys 2015;51:177–85. doi:10.1134/S0001433815010089.
[27] Vigouroux C, Bauer Aquino CA, Bauwens M, Becker C, Blumenstock T, De Mazière M, et al. NDACC harmonized formaldehyde time series from 21 FTIR stations covering a wide range of column abundances. Atmos Meas Tech 2018;11:5049–73. doi:10.5194/amt-11-5049-2018.
[28] Hase F, Hannigan JW, Coffey MT, Goldman A, Höpfner M, Jones NB, et al. Intercomparison of retrieval codes used for the analysis of high-resolution, ground-based FTIR measurements. J Quant Spectrosc Radiat Transfer 2004;87:25–52.
[29] Hase F, Wallace L, McLeod SD, Harrison JJ, Bernath PF. The ACE-FTS atlas of the infrared solar spectrum. J Quant Spectrosc Radiat Transfer 2010;111:521–8.
[30] Garcia RR, Marsh DR, Kinnison DE, Boville BA, Sassi F. Simulation of secular trends in the middle atmosphere, 1950–2003. J Geophys Res 2007;112:D09301. doi:10.1029/2006JD007485.